Analytical Methods

Highly reproducible electrochemical biosensor for Influenza A virus towards low-resource settings

Journal:	*Analytical Methods*
Manuscript ID	AY-ART-10-2023-001825.R1
Article Type:	Paper
Date Submitted by the Author:	21-Dec-2023
Complete List of Authors:	Ojeda, Julio; University of Central Florida, Chemistry Torres-Salvador, Fiorella; University of Central Florida, Chemistry Bruno, Nicholas; University of Central Florida, Chemistry Eastwood, Hannah; University of Central Florida, Chemistry Gerasimova, Yulia; University of Central Florida, Department of Chemistry Chumbimuni-Torres, Karin; University of Central Florida, Chemistry; UTSA,

ARTICLE

Highly reproducible electrochemical biosensor for Influenza A virus towards low-resource settings

Received 00th January 20xx,
Accepted 00th January 20xx

DOI: 10.1039/x0xx00000x

Julio Ojeda[a] , Fiorella Torres-Salvador[a], Nicholas Bruno[a], Hannah Eastwood[a], Yulia Gerasimova[a] and Karin Chumbimuni-Torres[a*]

Abstract. A highly reproducible electrochemical biosensor, employing a five-stranded four-way junction (5S-4WJ) system through square wave voltammetry, has been successfully validated for the detection of Influenza A virus (InfA). A comprehensive assessment of its linearity, precision, accuracy, and robustness has demonstrated its compliance with FDA standards. Integration with Nucleic Acid-Based Amplification (NASBA) has showcased its selectivity for InfA, enabling the detection of InfA RNA with a standard heater set at 41°C. This platform offers a straightforward setup well-suited for use at low-resource facilities.

A. Introduction

Seasonal Influenza is an acute respiratory infection caused by Influenza viruses. There are four types of Influenza: types A, B, C, and D. Influenza A and B viruses are the ones that circulate and cause seasonal epidemics.[1–3] In terms of transmission, seasonal Influenza spreads easily, with rapid transmission in crowded areas.[1,2] During periods of low Influenza activity and outside of epidemic situations, infections caused by other respiratory viruses, such as Rhinovirus, Respiratory syncytial virus, Parainfluenza, and Adenovirus, can also present as Influenza-like illness, making the clinical differentiation of Influenza from other pathogens difficult.[1]

For proper surveillance and control over the spread of respiratory viruses, many organizations like the World Health Organization (WHO) recommend the implementation of technologies at point of care (POC) settings.[4] Point-of-care testing (POCT) is referred to as a diagnostic procedure that can be conducted in proximity to or at the same location as the patients,[5] while maintaining both reliability and easy administration.[6]

Various methods have been proposed for diagnostics of Influenza.[7,8] Such as the detection of the viral antigen, which is exemplified by Rapid Influenza Diagnosis tests (RIDTs) or Immunofluorescence assays. These tests are characterized by short-to-moderate sample-to-result time; 15 min for RIDTs and 2-4 hours for immunoassays with high selectivity but low-to-moderate sensitivity. While both Influenza A and B viral antigens can be detected, such diagnostic methods are unable to further identify Influenza A virus subtypes.[9,10] To achieve higher selectivity and maintain high sensitivity and short turnaround time, Nucleic acid amplification tests (NAATs) through rapid molecular assays are used for upper respiratory tract specimens.[8] These tests employ Reverse Transcription-Polymerase Chain Reaction (RT-PCR) technology, which has high sensitivity and can produce results in approximately 20-30 minutes.[7,11] Although NAATs offer advantages compared to antigen testing, the requirement for sophisticated equipment and substantial infrastructure could pose challenges for POCT implementation in low-resource settings.[6]

Although RT-PCR has their respective strengths and limitations, electrochemical biosensors (E-biosensors) have shown certain advantages over them. As they offer portability that eliminates the need for sophisticated laboratory infrastructure; and low cost, allowing for the sensor to be employed in low-budget facilities while maintaining high analytical sensitivity and selectivity. [8,12,13] Thus numerous successful electrochemical platforms can be found for disease detection, such as of metal-organic frameworks coupled with screen-printed electrodes[14], homogeneous electrochemical sensors based on the in situ generation of electroactive substances[15], aptamer recognition system[16] , and DNA probes designed for specific sequence recognition.

As demonstrated previously, E-biosensors based on the four-way junction system (4WJ) allow for the selective detection of DNA and RNA fragments.[17–19] The 4WJ (Scheme 1) consists of a universal stem-loop strand (USL) attached to the electrode's surface and two strands (m and f) with target-complementary fragments, which are responsible for selectivity and the unraveling of the target's secondary structure, respectively. The m strand is covalently modified with a methylene blue (MeB) dye, which enables the electrochemical signal.[17,19,20]

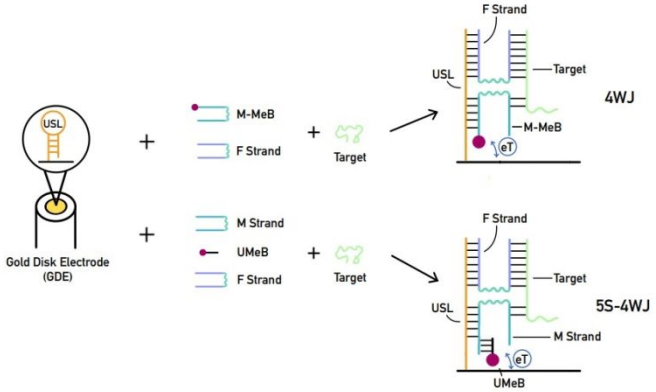

[a] Department of Chemistry, University of Central Florida, Orlando, FL 32816, US. karin.chumbimunitorres@ucf.edu

Electronic Supplementary Information (ESI) available: [details of any supplementary information available should be included here]. See DOI: 10.1039/x0xx00000x

Scheme 1. Scheme of the 4WJ and 5S-4WJ formation

These 4WJ E-biosensors can be coupled with an amplification technique to further improve selectivity and the limit of detection.[21] One of these amplification techniques is the Nucleic Acid Sequence-Based Amplification (NASBA) which selectively amplifies a specific RNA target and, does not require sophisticated equipment, making it suitable to be used at resource-limiting settings.[22]

Besides the development of the platform, proper statistical validation of a technology is essential for ensuring the accuracy and reliability of the analysis. It facilitates comparisons, identifies, and mitigates errors, and helps meet regulatory compliance, which is vital for future commercialization. The most prioritized parameters of analytical assays for validation, according to regulatory bodies, are linearity, precision (repeatability and reproducibility), accuracy, selectivity, and robustness.[23–25] The proper validation of the E-biosensor is crucial for ensuring its reliability, which in turn facilitates the widespread use of DNA-based sensing platforms.

In this study, we have developed a modular electrochemical biosensor for the detection of Influenza A virus (InfA). Besides the USL, the sensor design includes a universal MeB-containing strand (UMeB), with a sequence that is independent of the target's but complementary to the m strand. This system, the 5 strands-4WJ (5S-4WJ), has been shown to reduce the cost of the most expensive components, the electrode-attached USL strand and MeB-conjugated signal reporter.[26,27] When combined with NASBA, this platform allows for the specific detection of InfA RNA fragments. The performance of the E-biosensor was validated following statistical parameters required by regulatory agencies, including linearity, precision, accuracy, and robustness. In addition, the efficiency of the NASBA procedure was evaluated using different experimental setups and instrumentation. The efficient amplification of a viral RNA fragment using a simple laboratory heater system at a single temperature makes the platform suitable for use at resource-limiting facilities, where sophisticated temperature control equipment may not be available.

B. Experimental Section

B.1 Chemicals and materials. Oligonucleotides used as NASBA primers, E-biosensor adapter strands, and synthetic target fragments were purchased from Integrated DNA Technologies (Coralville, IA). The sequences of all oligonucleotides are listed in Table S1. The NASBA Liquid kit was obtained from Life Sciences (St Petersburg, Fl) and contained 3xReaction Buffer (NECB-1-24), 6xNucleotide Mix (NECN1-24), 4xEnzyme Cocktail (NEC-1-24). Genomic RNA from Influenza A Virus, A/Wisconsin/67/05 (HA, NA) x A/Puerto Rico/8/34 (H3N2), Reassortant X-161B-NR-10045 was obtained through the NIH Biodefense and Emerging Infections Research Resources Repository, NIAID (Manassas, VA). Agarose powder and SYBR Safe DNA gel stain were obtained from Thermo-Fisher Scientific (Waltham, MA). S1000TM Thermal Cycler Bio Rad Laboratories, Inc (Hercules, CA, USA) and Mini Dry Bath with Heated Lid (Heater) from Thermo-Fisher Scientific (Waltham, MA) were used for NASBA. 6-mercapto-1-hexanol (MCH), Tris-HCl, MgCl2, and tris(2-carboxyethyl) phosphine hydrochloride (TCEP) were purchased from Sigma-Aldrich (St. Louis, MO). Sulfuric acid, NaCl, and NaOH were purchased from Fisher Scientific (Pittsburgh, PA). Gold disk electrodes (GDEs) were purchased from CH Instruments (Austin, TX). Alumina slurry was obtained from Buehler (Lake Bluff, IL). The immobilization buffer (IB) was prepared with 250 mM NaCl, 50 mM Tris-HCl, and adjusted to a pH of 7.4 using 1.0 M NaOH. The hybridization buffer (HB) was prepared with 100 mM NaCl, 50 mM Tris-HCl, 50 mM $MgCl_2$, and adjusted to a pH of 7.4 using 1.0 M NaOH.

B.2 Electrochemical measurement. Electrochemical measurements, such as square-wave voltammetry (SWV) and cyclic voltammetry (CV), were performed using a CHI660D Electrochemical Workstation and a CHI1230B Hand-held Electrochemical Workstation for reproducibility studies. A conventional three-electrode configuration was employed, comprising of a GDE as the working electrode, a platinum wire as the auxiliary electrode, and a silver/silver chloride (Ag/AgCl) reference electrode (shown in Figure S1). SWV measurements were conducted in 10 mL of the hybridization buffer (HB) within the potential range of 0.0 to -0.5 V, with a frequency of 100 Hz, an amplitude of 70 mV, and a step potential of 3 mV. Prior to the measurements, the HB solution was purged with nitrogen for 10 minutes to eliminate any dissolved oxygen. All measurements were performed in triplicate at a temperature of 25 °C.

B.3 E-Biosensor preparation. To clean the GDEs, they were first cleaned by placing them in a piranha solution (1:3 ratio of 30% H_2O_2 to 95%-98% H_2SO_4. Caution: The piranha solution is highly corrosive and should be handled with care) for 10 minutes. Subsequently, the GDEs were polished on a microcloth with 1.0, 0.3, and 0.05 μm alumina slurry and sonicated in ethanol and water for 2 minutes each to remove any residual alumina particles. The GDEs were then activated via CV in 0.5 M H_2SO_4 from 1.6 to -0.1 V for 10 cycles at a scan rate of 100 mV/s. The electrochemically active area of the GDEs was calculated using the gold reduction peak from the CV measurement.

To modify the GDE surface with the USL strand, its 5'-terminal thiol group was reduced with 1.0 mM TCEP by shaking the solution for 1 hour at 25 °C. The USL solution was then diluted to 0.1 μM using IB, and 15 μL of this solution was drop-casted onto each electrode and incubated for 30 minutes at 25 °C. Next, a solution of 15 μL containing 2 mM MCH in IB was drop-casted onto each electrode and incubated for 30 minutes at 25°C. This step helps prevent nonspecific absorption on the gold surface. The electrodes were then rinsed with IB and dried using nitrogen gas.

Before the hybridization of the E-biosensor with the DNA or RNA target, a baseline signal was established using SWV, as described above. This step allows for the determination of the initial electrochemical signal before target binding.

To form the 5S-4WJ structure, a hybridization solution was prepared. This solution consisted of 0.5 μM f-strand, 0.1 μM m-strand, 0.25 μM UMeB probe, and various concentrations of the synthetic InfA DNA target (Table S1) or 10% (v/v) NASBA amplicon of the viral RNA in the hybridization buffer (HB). Next, 15 μL of the hybridization solution was drop-casted onto each electrode and allowed to incubate for 30 minutes at 25°C.

After incubation, the electrode was rinsed with HB to remove any unbound molecules. The electrode's response to the hybridization is expressed as the current density peak (Jp) obtained from SWV. The current density peak is calculated by subtracting the baseline current (pre-hybridization) from the current post-hybridization and dividing it by the electrochemically active area of the electrode. This normalization allows for the comparison of results between different electrodes and experiments.

B.4 Electrochemical Characterization of E-Biosensor

To characterize the E-Biosensor, a CV was performed in HB buffer from -0.1 to 0.6V for 10 cycles at a scan rate of 1 V/s. The HB solution

was purged with nitrogen to remove dissolve oxygen. The GDE, GDE casted with USL and MCH and GDE with the 5S-4WJ was tested.

B.5 Electrochemical performance of E-Biosensor. To optimize the E-biosensor performance, InfA DNA target corresponding to the sensor-interrogated fragment of the Influenza A M-gene was used. First, hybridization time was optimized by evaluating the E-biosensor response after 1, 5, 10, 15, 30, 45, and 60-minute hybridization with a 50nM InfA DNA target.

B.5.1 Linearity assessment. To establish the linear range of the E-biosensor, InfA DNA target was used at a concentration range between 0 and 60 nM. Three calibration curves were constructed using different concentrations of InfA DNA target. To validate the linearity of the calibration curve, an F-test was performed. The F-test compares the Fisher variance ratio between the lack-of-fit variance and the purely experimental variance (F calculated) against the critical value of F at a 95% confidence level (F tabulated). For the calibration curve to be considered linear, the F calculated value must be lower than the F tabulated value. This condition ensures that the lack-of-fit variance is not significantly greater than the experimental variance, indicating a good fit of the data to the linear calibration curve.[24] The regression analysis was performed using Minitab 16 software.

B.5.2 Limit of detection and quantification. The limit of detection (LOD) was calculated using the formula LOD = 3.0 x σBlank / slope, where σBlank represents the standard deviation of the blank measurements, and slope refers to the slope of the calibration curve. This calculation provides a threshold value, at which the signal can be reliably distinguished from the background noise, indicating the lowest concentration of the target analyte that can be detected by the E-biosensor.

Similarly, the limit of quantification (LOQ) was assessed using the formula LOQ = 10 x σBlank / slope. The LOQ represents the lowest concentration of the target analyte that can be quantified with acceptable precision and accuracy. It takes into account the noise level of the blank measurements and the slope of the calibration curve to establish a reliable quantification threshold.

B.5.3 Precision (repeatability, reproducibility). The repeatability of the method was assessed by conducting ten replicates at four different concentration levels: a lower level (1 nM and 2.5 nM), an intermediate level (15 nM), and a higher level (25 nM). All the replicates were performed by the same analyst on the same day using the same equipment.

Reproducibility was evaluated by conducting ten replicates at the same concentration levels as the repeatability assessment. However, for reproducibility, the replicates were performed by two different analysts on different days and using different types of equipment (either bench-top or hand-held electrochemical Workstation).

The standard deviation or repeatability (Sr) and reproducibility (SR) were employed to compute the relative standard deviation (RSD) for both repeatability and reproducibility. These RSD values were then compared with the guidelines set by the Food and Drug Administration (FDA).

B.5.4 Accuracy. To assess the accuracy of the method, ten replicates were conducted at three different target concentrations (2.5, 15, and 25 nM). All the replicates were performed by the same analyst on the same day using the same equipment. The concentration of the target was measured based on the electrochemical signal and using the calibration curve obtained during the linearity assessment.

The percent recovery was calculated for each replicate by comparing the measured concentration to the expected concentration. This indicates how accurately the method can recover the target concentration.

To determine if there were any statistical differences in the percent recoveries at each concentration level, a one-way analysis of variance (ANOVA) was performed. This analysis provides insights into the accuracy and consistency of the method across different target concentrations.

B.5.5 Robustness. The robustness tests were conducted using the Youden and Steiner partial factorial model,[28,29] which involved deliberately changing three factors from their normal conditions. The selected factors for the experiment were pH, temperature, and Mg^{2+} concentration in the hybridization buffer. For each factor, a high (+) and low (-) value was established, with a variation of ±10% to temperature, Mg^{2+} concentration, and either ±10% (Test 1) or ±5% (Test 2) of the pH from the standard conditions. The concentration of InfA DNA target for both variation ranges were kept at 25 nM. The experimental design, as shown in Table 1, consisted of eight experiments, each representing a different combination of the factor values. Three replicates were performed for each experiment to obtain average values (Ri) for analysis.

These tests aimed to evaluate the impact of parameter variations on the performance and reliability of the method.

Table 1. Youden and Steiner model for testing robustness of the InfA E-biosensor

Test 1	Experiment							
Factor	1	2	3	4	5	6	7	8
pH	8.14	8.14	8.14	8.14	6.66	6.66	6.66	6.66
Temperature	27.5	27.5	22.5	22.5	27.5	27.5	22.5	22.5
Mg^{2+} (mM)	55	45	55	45	55	45	55	45
Result (nM)	R1	R2	R3	R4	R5	R6	R7	R8
Test 2	Experiment							
Factor	1	2	3	4	5	6	7	8
pH	7.77	7.77	7.77	7.77	7.03	7.03	7.03	7.03
Temperature	27.5	27.5	22.5	22.5	27.5	27.5	22.5	22.5
Mg^{2+} (mM)	55	45	55	45	55	45	55	45
Result (nM)	R1	R2	R3	R4	R5	R6	R7	R8

B.5.6 Shelf-life evaluation. To evaluate the stability of the USL and MCH bonding on the gold surface of the electrodes, a series of electrodes were prepared up to the step of MCH attachment, as described in section 2.3 above. These electrodes were then stored at either -20 °C or 4 °C for three weeks. Every week, the stored electrodes were tested by performing the hybridization with a 25nM InfA DNA target for a hybridization time of 10 minutes. To assess any significant differences in the performance of the electrodes over time, a t-test was conducted. The average results from three electrodes per test were compared to evaluate any changes in the E-biosensor response. This allowed for the evaluation of degradation and/or changes in the E-biosensor response over time.

B.6 NASBA reaction. Genomic RNA from the Influenza A virus was used as a template for NASBA amplification of the M1 protein gene at a 10-fold dilution. The previously published primers InfA_MP_S778-4 and InfA_MP_A979 [30] were used for the NASBA reaction. The reaction was performed using the NASBA Kit, following

the vendor-recommended protocol with slight modifications. Samples were prepared by mixing 1 µL of the RNA template dilution with 4 µL of the 3x Reaction Buffer, and 2 µL of a 6X Nucleotide Mix to a total volume of 9 µL. The samples were incubated at 65 °C for 2 minutes, followed by incubation at 41 °C for 10 minutes. Then, 3 µL of the 4xEnzyme Cocktail was added to the reaction, and the samples were incubated at 41 °C for 90 minutes using a BioRad S1000 Thermal Cycler. Control samples, including a non-target control (NTC) with water instead of RNA template and a negative control (NC) with Influenza B (InfB) instead of Influenza A, were included in all experiments. To test if a simplified NASBA protocol avoiding the use of a thermocycler can be employed, the amplification reaction was performed using a heater at the same temperatures as described above. Subsequently, the 65°C annealing step was eliminated to streamline the protocol. The amplicons were obtained using either thermocycler-assisted two-step temperature protocol, heater-assisted two-step temperature protocol, or heater-assisted one-step temperature protocol and were analyzed by gel electrophoresis on a 2% agarose containing SYBR Safe DNA gel stain and visualized using a Bio-Rad Gel Doc XR+ with Image Lab software. In parallel, the amplicons were tested using the E-biosensor, with the analysis performed in triplicates. A paired t-test was employed to assess the variation of 3 replicates after each NASBA protocol.

C. Results and Discussion

C.1 Electrochemical performance of Influenza A E-biosensor. The response of the InfA E-biosensor was evaluated on GDEs using a DNA fragment corresponding to the InfA M1 gene (InfA DNA Target, Table S1). M1 gene was selected to enable the detection of all Influenza A serotypes.[12]

To determine the optimal hybridization time for efficient binding of InfA DNA target, a series of experiments were conducted (Fig. S2). It can be observed that the E-biosensor response reaches saturation at 45 minutes of hybridization. However, even at the incubation time as low as 5 min, the target-dependent signal can be distinguished from the blank (Figure S2 inset). To ensure efficient binding of the target to the sensor and, at the same time, to minimize the overall assay time, a hybridization time of 30 minutes was selected for all subsequent experiments.

In previous work, ellipsometry measurements have demonstrated that the thickness of the immobilized USL probe on gold surfaces aligns with our assumption of the stem-loop folded conformation of the USL probe.[17] CV measurements illustrated that upon casting the GDE with USL and MCH, there is a significant decrease in charge due to the passivation of the surface. Subsequently, once the 5S-4WJ structure is formed, the redox peak of the MeB appears.

The response of the InfA E-biosensor to varying concentrations of InfA DNA target was evaluated within the range of 0 to 60 nM. To establish the linear range, in addition to computing the R^2 value, an F test between the lack-of-fit variance and the purely experimental variance was performed to assess the statistical significance of the linear regression across the ranges of 2.5-25nM (Table S2), 2.5-40nM (Table S3), and 1-25nM (Table S4). Between the range of 2.5 to 25 nM, Figure 1 shows an R^2 value of 0.99. This indicates a strong correlation between the concentration of the InfA target and the E-biosensor response within this range. To assess the statistical significance of the linear regression,[24] an F test was conducted. The F test confirmed a statistically significant regression for the 2.5-25 nM range (Ftable = 4.96 < Fc = 697.18) (Table S2), indicating a statistically significant relationship between the concentration of the InfA target within this range and the E-biosensor response. Furthermore, the lack of fit was found to be non-significant (Fc = 1.96 < Ftable = 3.71), suggesting that the linear model adequately represents the data. The limit of detection (LOD) and limit of quantification (LOQ) were calculated as 0.34 nM and 1.04 nM, respectively.

For the linear regression analysis between 2.5 to 40 nM target, the R^2 value for the corresponding calibration curve was found to be 0.98 (Figure S4A). However, the lack of fit calculation (Table S3) was found to be significant (Fc = 14.70 > Ftable = 3.71), indicating that the linear model may not be the best fit for describing this system. This shows that even when the R^2 value is close to 1 (as 0.99 and 0.98 in these cases), the lack of fit test must be performed to choose the best range to apply a linear model.

While assessing the calibration curve from 1 to 25 nM, the R^2 value of 0.99 was attained (Figure S4B), with a LOD and LOQ of 0.33 nM and 0.99 nM, respectively. Moreover, both the regression analysis and lack-of-fit test also passed the statistical F test, as indicated in Table S4. However, it is noteworthy that when examining the reproducibility at 1 nM target concentration, a relative standard deviation of reproducibility (RSDR) of 38.25% was obtained (see Table 2), which surpasses the accepted FDA threshold of 25% near the LOQ.[31] Consequently, to conform with FDA guidelines, our evaluation was set in the range of 2.5 to 25 nM.

This highlights the importance of not solely relying on a calibration curve with an R2 value nearing 1 and a favorable F test outcome for regression and lack of fit. It is imperative to additionally consider other validation parameters outlined in the reference guidelines to accurately define the operational range.

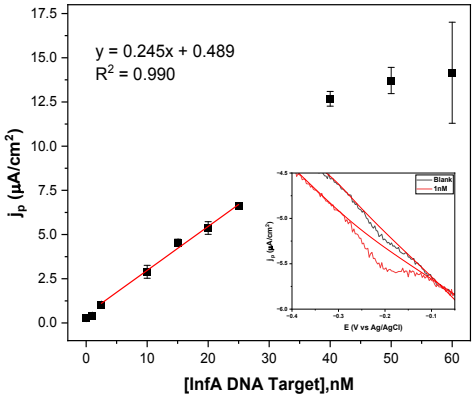

Figure 1. Response of the InfA E-biosensor to different concentrations (0, 1, 2.5, 10, 15, 20, 25, 40, 50, 60 nM) of InfA DNA target on GDEs with a 30-min hybridization time. Red line shows a linear trendline within 2.5-25 nM concentration range. Inset: SWV response of the blank (black) and sample containing 1 nM target (red) with their respective baselines.

The precision analysis of the E-biosensor was followed at three target concentrations, spanning the entire set linear range of the calibration curve (2.5, 15, and 25 nM). The relative standard deviation of repeatability (RSDr) and reproducibility were consistently below 25%, regardless of the target concentration tested (Table 2). These results align with the guidelines set by the FDA, which suggests a tolerable 20% variation for ligand binding assays such as immunoassays, and up to a 25% variation near the LOQ.[31] It is fair to

clarify that currently, to the best of our knowledge, there are no agency guidelines specifically tailored for electrochemical biosensors. Therefore, there are no regulated or standardized acceptance criteria in terms of percentage variation. However, in the absence of specific guidelines, it is common to refer to general guidelines as a reference for assessing the precision of electrochemical biosensors.

Table 2. Analysis of repeatability and reproducibility of the Influenza A E-Biosensor

[InfA DNA target]	Sr	SR	RSDr	RSDR
1 nM	0.24	0.33	26.49	38.25
2.5 nM	0.41	0.56	16.42	24.40
15 nM	1.80	2.25	11.81	14.07
25 nM	2.54	3.32	10.43	13.62

Sr: Standard deviation for repeatability, SR: Standard deviation for reproducibility, RSDr: Relative standard deviation of repeatability, RSDR: Relative standard deviation of reproducibility.

To evaluate accuracy, three concentrations were examined, representing the lower, middle, and higher ends of the calibration range. Utilizing the calibration curve equation, the current density signal was converted into concentration, allowing for the calculation of percent recovery relative to the anticipated concentration. The results indicated a recovery percentage falling between 97% and 101% (Table 3), aligning with FDA criteria for accuracy, as it falls within the ±20% range.[31] ANOVA calculations were utilized (as shown in Table S5) to ascertain the consistency of recovery percentages across the three levels within the linear range. The results confirmed their statistical equivalence, implying a consistent maintenance of accuracy across this range.

Table 3. Analysis of the Influenza A E-biosensor accuracy

Concentration	Average ± S. Deviation (10)	% Recovery
2.5 nM	2.49 ± 0.41	99.56
15 nM	15.21 ± 1.80	101.37
25 nM	24.39 ± 2.54	97.54

The robustness test was performed by allowing a ±10% variation of such parameters as pH, temperature, and magnesium ion concentration of the buffer. These parameters were chosen because will affect the duplex stability of the 5S-4WJ structure, and therefore the capability of generating signal. The electrochemical signal obtained for each of the tested conditions at 25 nM InfA DNA target was converted to the target concentration calculated based on the calibration curve shown in Figure 1. The calculated concentrations are listed in Table S6. The effect of each factor is calculated with the following formula:

$$Effect\ (A) = \left|\sum R(A+) - \sum R(A-)\right|/2$$

Where R(A+) is the result from the experiment where factor A has a higher value, and, in the same way, R(A-) where factor A has a lower value according to Table 1. A factor would be considered to have a significant effect if it exceeds the value of 1.4 times SR (limit of acceptance)[28]. Based on that, as can be seen in Table 4, the robustness test showed a significant effect from pH, followed by a non-significant effect from temperature and Mg^{2+} concentration.

Table 4. Robustness test results from evaluation at ±10% variation of all parameters at 25 nM InfA DNA target

Factor	Variable	Sum	Effect	Limit of acceptance	Effect (%)
pH	8.14	107.21	10.97	4.70	20.46
	6.66	85.27			
Temperature (°C)	27.5	93.05	3.19	4.70	6.86
	22.5	99.43			
Mg^{2+} (mM)	55	96.95	0.72	4.70	1.48
	45	95.52			

To further investigate the impact of pH on the results, the E-biosensor was tested in the presence of 2.5 nM or 25 nM InfA DNA target by varying the pH from 6.66 to 8.14 while keeping the other assay parameters constant (room temperature at 25 °C and 50 mM of Mg^{2+} in the HB buffer). It was observed that the signal decreased at pH<7.4 and slightly increased at pH >7.4 (Figure 2). At this pH range, a change in the ionization state of nucleotide functional groups is not expected as this would require a pH below 5 and above 9.[32] Therefore, destabilization of the 5S-4WJ structure is unlikely within such small changes in pH. Even though the buffering capacity of the HB (based on tris-HCl) is from 7 to 9.[33] Which indicates that at 6.66 a proper buffer will not be formed, the pH was tested before each measurement to confirm the pH value did not change beyond what was expected.

Since the reduction of MeB requires two electrons and one proton,[34] the reduction potential of MeB would depend on pH and is expected to be more positive at lower pH. We compared the effect of pH in the reduction potential of MeB in the range of 6.66-8.14 for a solution of methylene blue (32 ⍰M) and an E-biosensor containing 0.25 ⍰M UMeB strand as part of the 5S-4WJ structure (Figure S5). Indeed, the reduction potential was inversely proportional to pH with a linear relationship similar for both systems. This suggests that the pH effect is attributed to the MeB marker rather than to the DNA strand interactions.

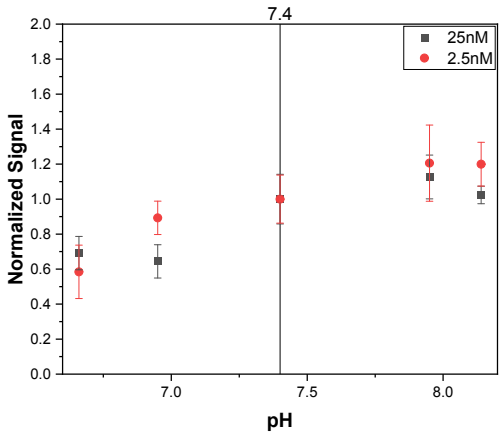

Figure 2. Normalized response of the InfA E-biosensor to different pH at 2.5 nM (black dots) or 25 nM (red dots) InfA DNA target using GDE at a 30-min hybridization time.

For all these reasons, the variation of pH was decreased from ±10% to ±5%, and the robustness test was repeated (table 5, table S7). In this range, the method is robust toward pH variation, confirming that the 5S-4WJ InfA E-biosensor is robust under these conditions.

Table 5. Robustness test results at ±10% variation for Mg^{2+} concentration and temperature, and at ±5 % variation for pH

Factor	Variable	Sum	Effect	Limit of acceptance	Effect (%)
pH	7.77	93.68	2.27	4.70	4.83
	7.03	89.15			
Temperature (°C)	27.5	91.36	0.06	4.70	0.12
	22.5	91.47			
Mg^{2+} (mM)	55	88.72	2.70	4.70	6.09
	45	94.12			

Next, the shelf life of the USL/MCH-modified electrodes was assessed. As shown in Figure S6A, when the electrodes were kept at -20°C, the target-triggered response of the E-biosensor remained statistically similar (at a 95% confidence level) for 21 days. On day 21, the coefficient of variation reached 20%, which was the highest value observed during the assessment period. However, it can be concluded that the GDEs cast with USL and MCH can withstand storage in the freezer for up to 21 days while maintaining a consistent response. In Figure S6-B, it was observed that storing the electrodes at 4°C resulted in a decrease in signal over time, with a loss of 26% of the signal over a period of 14 days. Although the t-test between day 0 and day 14 for this experiment did not show a significant difference, the clear downward trend indicates that these temperature conditions are affecting the stability of the USL on the gold surface, therefore the 4°C is not a suitable condition for storing USL/MCH-modified GDEs for the E-biosensor assay.

To use the E-biosensor in clinical practice, the interrogated fragment of InfA RNA should be amplified to exceed the LOD and LOQ values of the system. Here, we selected NASBA as an isothermal RNA amplification method. Different NASBA setups were tested: (1) a thermocycler-assisted NASBA performed in a two-step setup, with 65 °C annealing and 41 °C amplification steps (PC); (2) a heater-assisted NASBA in a two-step setup, 65 °C and 41 °C (H-2); and (3) a heater-assisted NASBA in a one-step setup omitting the annealing step, keeping just the 41 °C step (H-1). Regardless of the setup used, an amplicon of 210 nts was obtained (Figure S7). Correspondently, no statistically significant difference was observed in the response of the E-biosensor towards the InfA amplicons obtained using the three NASBA setups (Figure 3), according to the unpaired t-test. This suggests that the E-biosensor assay can be implemented using a simpler one-step protocol (reaction at 41°C only) utilizing an inexpensive heater affordable for even low-resource laboratory or testing facility. The amplification was also shown to be specific for InfA RNA. As expected, in the absence of an RNA template (NTC), no amplicon was produced, resulting in a low signal. Additionally, when RNA from the Influenza B virus was used as a template (NC), no amplification and low signal were observed (Figure S7, Figure 3).

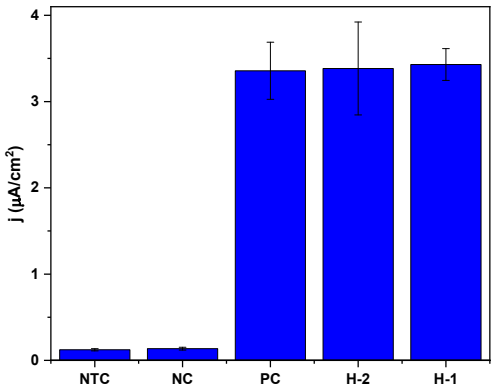

Figure 3. Response of the InfA E-biosensor to the amplicons obtained using different NASBA setups. NTC: NASBA No-template control, NC: Negative control (InfB RNA used as a template), PC: Positive control (INf A RNA used as a template for the thermocycler-assisted NASBA with two temperature steps), H-2: NASBA using InfA RNA in a heater with two temperature steps, H-1: NASBA using InfA RNA in a heater with only 41 °C reaction temperature used.

Conclusions

In summary, this study successfully validated a DNA E-biosensor based on the 5S-4WJ system, demonstrating its efficacy for the detection of Influenza A genetic signatures. The calibration curve was statistically evaluated within the 2.5 to 25nM range of a DNA sequence mimicking the interrogated fragment of the viral genome. Moreover, precision and accuracy align with FDA standards, affirming the applicability and feasibility of implementing this platform in resource-limiting settings.

Furthermore, the robustness test uncovered that pH variations of ±10% can significantly impact the results due to their effect on the methylene blue dye, additionally to the lack of buffer capacity below 7 for a tris-HCl based buffer. Hence, maintaining pH within ±5% and, Mg2+ concentration and temperature within ±10% ranges is essential when utilizing this platform. By coupling the E-biosensor with NASBA, it becomes feasible to detect Influenza A RNA amplicons using a standard heater, set to just 41°C. This streamlined setup holds promise for InfA testing at low-resource diagnostic facilities, simplifying detection procedures.

Author Contributions

K.C.T., J.O. conceived and planned the work. F.T.S. implemented the NASBA protocol. J.O., F.T.S., N.B., H.E. conduct-ed experiments and analysed the results. Y.G., K.C.T. supervised the project. J.O. wrote the initial draft of the manuscript with contributions from all authors. J.O., F.T.S., N.B., H.E., K.C.T., Y.G. edited.

Conflicts of interest

There are no conflicts to declare.

Acknowledgements

Funding from the National Science Foundation (1706802) and the National Institutes of Health (R03AI164938) are greatly appreciated. Genomic RNA from Influenza A was deposited by the Centers for Disease Control and Prevention and obtained through BEI Re-sources.

Notes and references

1 Influenza (Seasonal), https://www.who.int/news-room/fact-sheets/detail/influenza-(seasonal), (accessed 2 August 2023).
2 Y. Amano and Q. Cheng, Detection of influenza virus: traditional approaches and development of biosensors, *Anal. Bioanal. Chem.*, 2005, **381**, 156–164.
3 L. Krejcova, D. Hynek, V. Adam, J. Hubalek and R. Kizek, Electrochemical Sensors and Biosensors for Influenza Detection, *Int. J. Electrochem. Sci.*, 2012, **7**, 10779–10801.
4 Global partnership to make available 120 million affordable, quality COVID-19 rapid tests for low- and middle-income countries, https://unitaid.org/news-blog/global-partnership-to-make-available-120-million-affordable-quality-covid-19-rapid-tests-for-low-and-middle-income-countries/, (accessed 7 August 2023).
5 ISO 15189:2022(en), Medical laboratories — Requirements for quality and competence, https://www.iso.org/obp/ui/en/#iso:std:iso:15189:ed-4:v1:en, (accessed 7 August 2023).
6 N. P. Pai, C. Vadnais, C. Denkinger, N. Engel and M. Pai, Point-of-Care Testing for Infectious Diseases: Diversity, Complexity, and Barriers in Low- And Middle-Income Countries, *PLoS Med.*, 2012, **9**, e1001306.
7 Overview of Influenza Testing Methods | CDC, https://www.cdc.gov/flu/professionals/diagnosis/overview-testing-methods.htm, (accessed 2 August 2023).
8 P. P. Nelson, B. A. Rath, P. C. Fragkou, E. Antalis, S. Tsiodras and C. Skevaki, Current and Future Point-of-Care Tests for Emerging and New Respiratory Viruses and Future Perspectives, *Front. Cell. Infect. Microbiol.*, 2020, **10**, 181.
9 Influenza Signs and Symptoms and the Role of Laboratory Diagnostics | CDC, https://www.cdc.gov/flu/professionals/diagnosis/labrolesprocedures.htm, (accessed 2 August 2023).
10 Information for Clinicians on Rapid Diagnostic Testing for Influenza | CDC, https://www.cdc.gov/flu/professionals/diagnosis/rapidclin.htm, (accessed 2 August 2023).
11 Information on Rapid Molecular Assays, RT-PCR, and other Molecular Assays for Diagnosis of Influenza Virus Infection | CDC, https://www.cdc.gov/flu/professionals/diagnosis/molecular-assays.htm, (accessed 2 August 2023).
12 Z. Zhao, C. Huang, Z. Huang, F. Lin, Q. He, D. Tao, N. Jaffrezic-Renault and Z. Guo, Advancements in electrochemical biosensing for respiratory virus detection: A review, *TrAC Trends Anal. Chem.*, 2021, **139**, 116253.
13 Y. Tepeli and A. Ülkü, Electrochemical biosensors for influenza virus a detection: The potential of adaptation of these devices to POC systems, *Sens. Actuators B Chem.*, 2018, **254**, 377–384.
14 X. Liu, X. Gao, L. Yang, Y. Zhao and F. Li, Metal–Organic Framework-Functionalized Paper-Based Electrochemical Biosensor for Ultrasensitive Exosome Assay, *Anal. Chem.*, 2021, **93**, 11792–11799.
15 L. Yu, J. Chang, X. Zhuang, H. Li, T. Hou and F. Li, Two-Dimensional Cobalt-Doped Ti_3C_2 MXene Nanozyme-Mediated Homogeneous Electrochemical Strategy for Pesticides Assay Based on In Situ Generation of Electroactive Substances, *Anal. Chem.*, 2022, **94**, 3669–3676.
16 L. Yang, X. Yin, B. An and F. Li, Precise Capture and Direct Quantification of Tumor Exosomes *via* a Highly Efficient Dual-Aptamer Recognition-Assisted Ratiometric Immobilization-Free Electrochemical Strategy, *Anal. Chem.*, 2021, **93**, 1709–1716.
17 D. M. Mills, P. Calvo-Marzal, J. M. Pinzon, S. Armas, D. M. Kolpashchikov and K. Y. Chumbimuni-Torres, A Single Electrochemical Probe Used for Analysis of Multiple Nucleic Acid Sequences, *Electroanalysis*, 2017, **29**, 873–879.
18 D. M. Mills, C. P. Martin, S. M. Armas, P. Calvo-Marzal, D. M. Kolpashchikov and K. Y. Chumbimuni-Torres, A universal and label-free impedimetric biosensing platform for discrimination of single nucleotide substitutions in long nucleic acid strands, *Biosens. Bioelectron.*, 2018, **109**, 35–42.
19 D. M. Mills, M. V. Foguel, C. P. Martin, T. T. Trieu, O. Kamar, P. Calvo-Marzal, D. M. Kolpashchikov and K. Y. Chumbimuni-Torres, Rapid detection of different DNA analytes using a single electrochemical sensor, *Sens. Actuators B Chem.*, 2019, **293**, 11–15.
20 M. Labib, S. M. Ghobadloo, N. Khan, D. M. Kolpashchikov and M. V. Berezovski, Four-Way Junction Formation Promoting Ultrasensitive Electrochemical Detection of MicroRNA, *Anal. Chem.*, 2013, **85**, 9422–9427.
21 C. A. Lynch, M. V. Foguel, A. J. Reed, A. M. Balcarcel, P. Calvo-Marzal, Y. V. Gerasimova and K. Y. Chumbimuni-Torres, Selective Determination of Isothermally Amplified Zika Virus RNA Using a Universal DNA-Hairpin Probe in Less than 1 Hour, *Anal. Chem.*, 2019, **91**, 13458–13464.
22 J. Compton, Nucleic Acid Sequence-Based Amplification, *Nature*, 1991, **350(6313)**, 91–92.
23 I. Taverniers, M. De Loose and E. Van Bockstaele, Trends in quality in the analytical laboratory. II. Analytical method validation and quality assurance, *TrAC Trends Anal. Chem.*, 2004, **23**, 535–552.
24 P. Araujo, Key aspects of analytical method validation and linearity evaluation, *J. Chromatogr. B*, 2009, **877**, 2224–2234.
25 T. N. Rao, in *Calibration and Validation of Analytical Methods - A Sampling of Current Approaches*, ed. M. T. Stauffer, InTech, 2018.
26 S.-C. Sun, H.-Y. Dou, M.-C. Chuang and D. M. Kolpashchikov, Multi-labeled electrochemical sensor for cost-efficient detection of single nucleotide substitutions in folded nucleic acids, *Sens. Actuators B Chem.*, 2019, **287**, 569–575.
27 A. Murray, J. Ojeda, O. El Merhebi, P. Calvo-Marzal, Y. Gerasimova and K. Chumbimuni-Torres, Cost-Effective Modular Biosensor for SARS-CoV-2 and Influenza A Detection, *Biosensors*, 2023, **13**, 874.

28 A.-G. Tenea, C. Dinu, G.-O. Buica and G.-G. Vasile, Electrochemical System for Field Control of Hg2+ Concentration in Wastewater Samples, *Sensors*, 2023, **23**, 1084.

29 E. Karageorgou and V. Samanidou, Youden test application in robustness assays during method validation, *J. Chromatogr. A*, 2014, **1353**, 131–139.

30 W. Xing, Y. Liu, H. Wang, S. Li, Y. Lin, L. Chen, Y. Zhao, S. Chao, X. Huang, S. Ge, T. Deng, T. Zhao, B. Li, H. Wang, L. Wang, Y. Song, R. Jin, J. He, X. Zhao, P. Liu, W. Li and J. Cheng, A High-Throughput, Multi-Index Isothermal Amplification Platform for Rapid Detection of 19 Types of Common Respiratory Viruses Including SARS-CoV-2, *Engineering*, 2020, **6**, 1130–1140.

31 FDA, Bioanalytical Method Validation Guidance for Industry.

32 G. M. Blackburn, M. J. Gait, D. Loakes and D. M. Williams, *Nucleic Acids in Chemistry and Biology*, Royal Society of Chemistry, 3rd edn., 2006.

33 Tris hydrochloride 1185-53-1, http://www.sigmaaldrich.com/, (accessed 27 August 2023).

34 E. Farjami, L. Clima, K. V. Gothelf and E. E. Ferapontova, DNA interactions with a Methylene Blue redox indicator depend on the DNA length and are sequence specific, *The Analyst*, 2010, **135**, 1443.